

Comparison of Standard Amplitude and Phase Compensation and Mutual Coupling Compensation in 60 GHz FMCW MIMO Radar

1st Djordje Stojiljkovic
Novelic
Belgrade, Serbia
0009-0009-0670-5996

2nd Djordje Glavonjic
Novelic
Belgrade, Serbia
0000-0003-0619-0151

3rd Lazar Janicijevic
Novelic
Belgrade, Serbia
0009-0000-1822-7623

4th Milan Stojanovic
Novelic
Belgrade, Serbia
0000-0002-1783-1615

5th Veljko Mihajlovic
Novelic
Belgrade, Serbia
0009-0003-1771-7278

Abstract—Numerous Frequency-Modulated Continuous-Wave (FMCW) radar applications require Angle Of Arrival (AOA) estimation through the use of antenna arrays. Due to manufacturing tolerances, the antennas not being ideal, and interference between the antennas, calibration is needed to achieve theoretical angular resolution. The most commonly used method is Amplitude and Phase Compensation (APC) which compensates the amplitudes and phases at reference angle. However, since this method does not take into account Mutual Coupling (MC) between the antennas, performance benefits of Mutual Coupling Compensation (MCC) algorithm over conventional APC are investigated. A model for MC is presented and two methods for MCC are evaluated. A dataset was created using an automated measurement system that sweeps through a range of angles to record the required measurement set needed for coefficient calculation. Radar corner reflector at fixed distance was used as a reference target. The results of the three methods (APC and two MCC) were evaluated for different positions of the reflector and different boards to determine performance relative to ideal theoretical response.

Index Terms—calibration, mutual coupling, angle of arrival, mutual coupling compensation, amplitude and phase compensation

I. INTRODUCTION

In MIMO FMCW radar systems, antenna arrays are widely used for estimating Angle Of Arrival (AOA) of various surrounding objects. There are multiple methods and approaches for determining AOA based on sensor array signals. Among them are conventional delay-and-sum beamformer (Bartlett's method) [1], Capon's method also known as Minimum Variance Distortion-less Response (MVDR) [2], Multiple Signal Classification (MUSIC) [3] and others. Mathematical foundations of these methods are based on assumptions about the expected signals received at the antenna array. The signal is expected to have complex sinusoidal model, and if this is satisfied, all methods are

This work was supported by Novelic.

achieving their theoretical performances. However, due to manufacturing differences and Mutual Coupling (MC) between the antennas, the resulting signal significantly differs from the reference one, which further increases angle estimation error and noise level. In order to compensate for these effects, calibration of radar system is required. The most commonly used calibration method is APC which is simple to implement, but may prove insufficient in high accuracy AOA applications. Therefore, a more complex Mutual Coupling Compensation (MCC) method is evaluated in this paper.

The purpose of this paper is to show the importance of calibration for AOA estimation and to present a comparison between APC and MCC calibration methods.

The paper is organized as follows. Theory of FMCW MIMO radars, APC and MCC methods is given in Section II. Later on, in Section III results of comparing different methods on 4 different datasets are shown. Finally, conclusions are presented in Section IV.

II. THEORY

FMCW radars use signals of varying frequency and most often utilize the linear frequency up-chirp signal [4]. In this way, received and sampled intermediate frequency signal, coming from a single target at a distance r , can be expressed as

$$s_{IF}[n] = A \cdot \exp \left[j \left(4\pi \frac{S}{cF_S} r \cdot n + 4\pi \frac{f_0}{c} r + \Phi_{\text{refl}} \right) \right], \quad (1)$$

where A is the amplitude of the signal, n is discrete time index, f_0 is chirp starting frequency, c is the speed of light, F_S is the sampling frequency, S is the slope of the chirp and Φ_{refl} is the phase shift due to reflection. There are N_S samples of a signal so the discrete time index n runs from 0 to $N_S - 1$. In case of MIMO radars there are multiple transmitting (Tx)

and multiple receiving (Rx) antennas. Basic model of acquiring FMCW MIMO radar signal is shown in Fig. 1. Due to difference in traveled distances, each antenna in virtual array receives different signal, as illustrated in Fig 1. This difference depends on incident angle θ . Assuming target is in the far field, this results in signals between consecutive antennas being different by constant steering factor $\exp\left[j2\pi\frac{f_0}{c}d \cdot \sin\theta\right]$ [5]. In Uniform Linear Array (ULA) with spacing d between the antennas, signal received at the m -th antenna is

$$s_{\text{IF}}[n, m] = \exp\left[j2\pi\frac{f_0}{c}d \cdot \sin\theta \cdot m\right] \cdot A \cdot \exp\left[j4\pi\frac{S}{cF_S}r \cdot n\right] \exp\left[j\left(4\pi\frac{f_0}{c}r + \Phi_{\text{refl}}\right)\right]. \quad (2)$$

Measured signals at a single time index from all antennas can be arranged in a vector

$$\mathbf{e} = \begin{bmatrix} s_{\text{IF}}[n, 0] \\ s_{\text{IF}}[n, 1] \\ \vdots \\ s_{\text{IF}}[n, M-1] \end{bmatrix} = \begin{bmatrix} 1 \\ e^{j2\pi\frac{f_0}{c}d \cdot \sin\theta} \\ \vdots \\ e^{j2\pi\frac{f_0}{c}d \cdot \sin\theta \cdot (M-1)} \end{bmatrix} s_{\text{IF}}[n, 0], \quad (3)$$

where M is the number of virtual antennas.

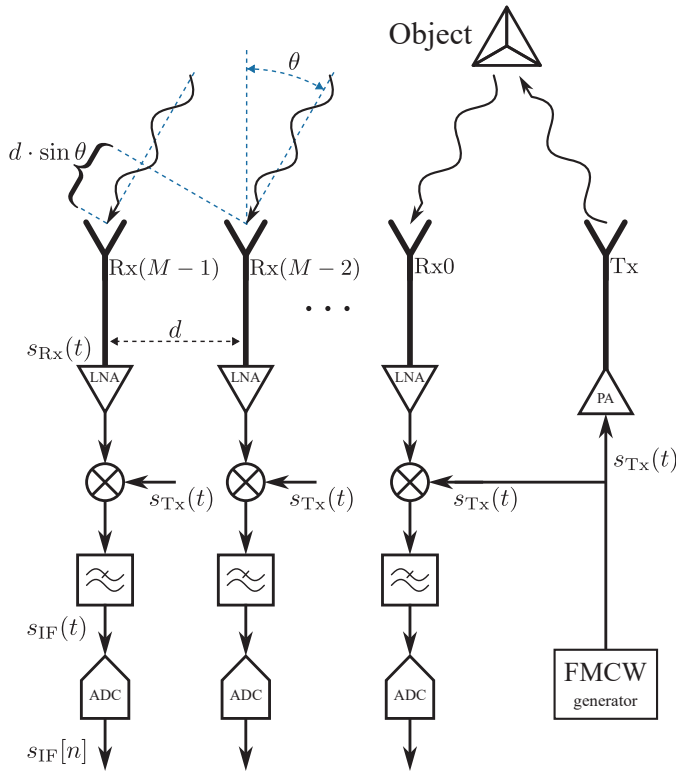


Fig. 1. Radar model and principle of AOA using multiple antennas.

A. Effects of Mutual Coupling

With the presence of multiple sensors in MIMO radars, the sensors experience mutual electromagnetic interference,

especially when they are close together. There are also manufacturing differences between the antennas. This causes the distortion in resulting angular pseudospectrums after performing AOA estimation, which increases angle estimation error and raises side lobes.

The mentioned effects represent MC and are modeled as a square matrix called Mutual Coupling Matrix (MCM) [6] which is denoted as \mathbf{C} . In this way signal received at m -th antenna is a linear combination of signals expected at all virtual antennas:

$$v[m] = \sum_{i=1}^{M-1} c_{im} E_i, \quad (4)$$

where E_i is expected signal at i -th antenna. Coefficients c_{im} are elements of \mathbf{C} . Mentioned effect is illustrated in Fig. 2.

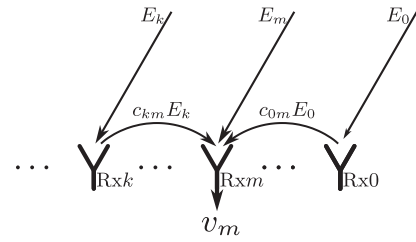


Fig. 2. Illustration of Mutual Coupling.

If a vector of signals \mathbf{e} is expected, due to MC, different vector of signals \mathbf{v} will be measured

$$\mathbf{v} = \mathbf{C}\mathbf{e}. \quad (5)$$

\mathbf{C} ($M \times M$) is a complex matrix and ideally should be equal to identity matrix, which would mean no MC is present. If a set of K measurements is taken, data vectors can be arranged in a matrix, and the signals will be distorted due to MC, giving a similar matrix equation

$$\mathbf{V} = \mathbf{C}\mathbf{E}, \quad (6)$$

where \mathbf{V} ($M \times K$) is the matrix of measured vectors corresponding to the matrix of expected vectors \mathbf{E} ($M \times K$). In order to compensate for MC effect and calibrate the radar system to receive the expected signal, inverse operation should be performed

$$\mathbf{E} = \mathbf{C}^{-1}\mathbf{V}. \quad (7)$$

B. Amplitude and Phase Compensation (APC)

Usually, the most prominent error in a MIMO radar system is caused only by manufacturing differences between the antennas, making them have different gains on the received signal and also adding different phase shifts. This error is present even at zero angle, where no differences in phase across the antennas should be seen. This error can be easily compensated by calibration. This calibration is performed by measuring a single target at zero angle giving a measurement vector \mathbf{v}_{APC} [7], [8]. Calibration of a new measurement vector \mathbf{v} is performed by element wise (Hadamard) division, giving

$$\mathbf{y} = \mathbf{v} \oslash \mathbf{v}_{\text{APC}}, \quad (8)$$

where \mathbf{y} is calibrated vector and \oslash represents the Hadamard division operator. This can be simply represented, using the MCM giving

$$\mathbf{y} = \mathbf{C}^{-1} \mathbf{v}, \quad (9)$$

with the MCM being

$$\mathbf{C} = \text{diag} \{ \mathbf{v}_{\text{APC}} \}. \quad (10)$$

This is equivalent of a system where no mutual interference between the antennas is present, but only each individual antenna's effect.

C. Mutual Coupling Compensation (MCC)

As described earlier, in order to compensate for MC effect MC matrix \mathbf{C} needs to be known or estimated. In order to calculate \mathbf{C} there are two similar methods considered in this paper [9], [10].

The majority of methods for estimating the MCM are based on measuring a single target at the same distance and K different angles. Using the signals that are expected at these angles, and the actual measured signals, MCM can be estimated. The measurements are most easily acquired by using a system containing rotating platform on which radar is mounted [11], as illustrated in Fig. 3. Radar is rotated around radar's center so that the center is always the same distance from the target. This method of recording measurements was used for acquiring necessary calibration datasets, which are analyzed in Sections III-A to III-B.

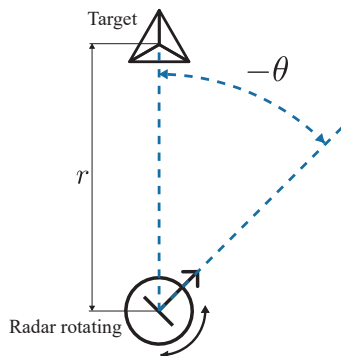


Fig. 3. Example of taking measurements by rotating the radar on a platform.

The method for estimating MCM, described in [9] considers solving the following optimization problem

$$\hat{\mathbf{C}} = \arg \min_{\mathbf{C}} \|\mathbf{V} - \mathbf{C}\mathbf{E}\|_F, \quad (11)$$

where $\|\cdot\|_F$ is the Frobenius norm of a matrix. A solution in the form of pseudoinverse is obtained as follows

$$\hat{\mathbf{C}} = \mathbf{V}\mathbf{E}^H (\mathbf{E}\mathbf{E}^H)^{-1}. \quad (12)$$

This method will be addressed as MCC1. In order to properly perform the estimation process, measurements need to be taken at K different angles with $K \geq M$. The pseudoinverse form in (12) gives a single solution in this case.

In [10] another method for estimating MCM is described. This method poses an optimization problem where array center offset and antenna radiation pattern are unknown. It uses an iterative process and estimates: antenna array center offset, antenna radiation pattern and MC matrix $\hat{\mathbf{C}}$. In the future, we will refer to this alternative approach as MCC2.

III. RESULTS

In order to demonstrate MCM estimation procedure and to show the effects of calibration on AOA estimation, several measurement sets were made using corner reflectors as targets. List of measurement datasets is in Table I.

TABLE I
ACQUIRED MEASUREMENT SETS

1	single target was placed at zero angle, and radar was mounted on the platform as in Fig. 3 (III-A)
2	single target was scanned at various distances from the radar for different AOAs (III-B)
3	single target was scanned using different radar boards in same scenario (III-C)
4	two targets with the same Radar Cross Section (RCS) were recorded at same distance and various AOAs (III-D)

Two different 60-GHz radar platforms were used for the measurements: IWR6843 having eight azimuth virtual antennas and BGT60ATR24C having four integrated virtual antennas.

For evaluating performance of angle estimation, conventional delay-and-sum beamformer was used [1]. This beamformer is used to derive angular pseudospectrum, which represents the distribution of signal power across different AOAs. Consequently, the AOA is determined by identifying the peak position in the angular pseudospectrum. These pseudospectrums are taken for single data frame, since all experiments were done in static environment.

As an example single measurement from dataset 1 in Table I was considered. Resulting angular pseudospectrums before and after performing calibration are shown in Fig. 4. By examining Fig. 4 it can be noted that:

- peak of the pseudospectrum is closer to the exact angle value;
- side lobes are diminished.

Error of AOA estimation and Side Lobe Level (SLL) can be calculated from pseudospectrums. Difference between estimated AOA and true angle value, represents error of estimation. The SLL denotes the difference between main lobe and highest side lobe, in decibels. When multiple measurements with different AOAs are given, error and SLL can be plotted for different azimuth AOAs. Furthermore, additional aggregate metrics can be obtained:

- Root Mean Square Error of AOA estimation - (RMSE_{AOA})
- mean of SLL as

$$\text{SLL}_{\text{mean}} = 10 \log_{10} \left[\frac{1}{K} \sum_{i=1}^K 10^{\frac{\text{SLL}_{\text{dB}}}{10}} \right]. \quad (13)$$

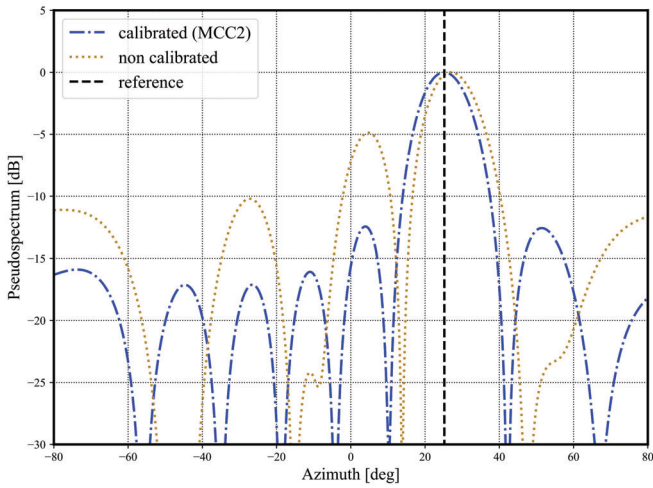


Fig. 4. Angular pseudospectrums before and after calibration.

A. Experiments with a single target

For single target experiments, radar was placed on a rotating platform in order to record a sweep of measurements in $[-60^\circ, 60^\circ]$ range with 1.8° step. IWR6843 was used for this procedure. Reflector having Radar Cross Section (RCS) of 4.19 was placed at the distance of 2m from radar, at zero angle. These measurements were used for estimating MCMs and APC coefficients and as single target scenarios. Experimental setup with radar on rotating platform, used for these measurements is given in Fig. 5.

After performing calibration, all calibration methods result in significantly improved pseudospectrum as shown in Fig. 6.

For these measurements AOA estimation error is given in Fig. 7 and SLL for different AOAs is given in Fig. 8. $RMSE_{AOA}$ and SLL_{mean} are presented in Table II. All three calibration methods reduce side lobes significantly. When considering estimation error, both MCC methods outperform APC, achieving error close to zero across all azimuth angles and having lower $RMSE_{AOA}$. APC shows larger error for AOAs beyond zero angle. MCC2 appears to have better estimation and lower side lobes than MCC1.

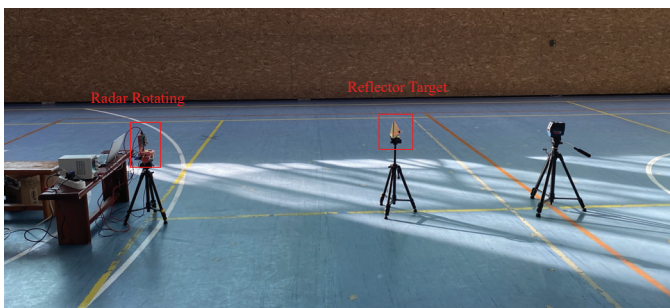


Fig. 5. Rotating radar setup.

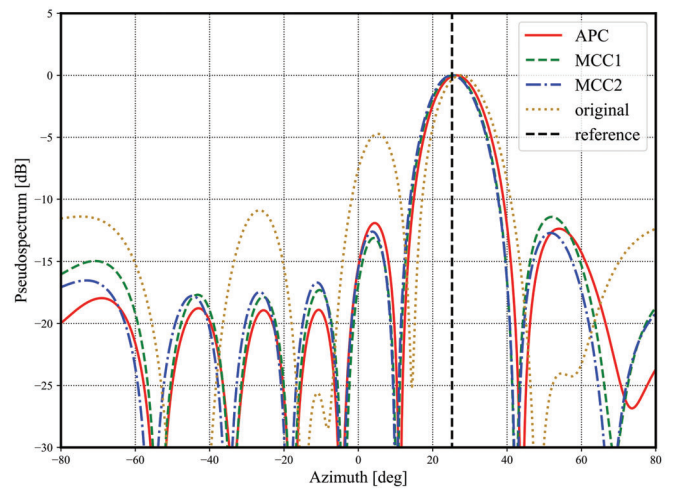


Fig. 6. Angular pseudospectrums for APC, MCC1 and MCC2 methods.

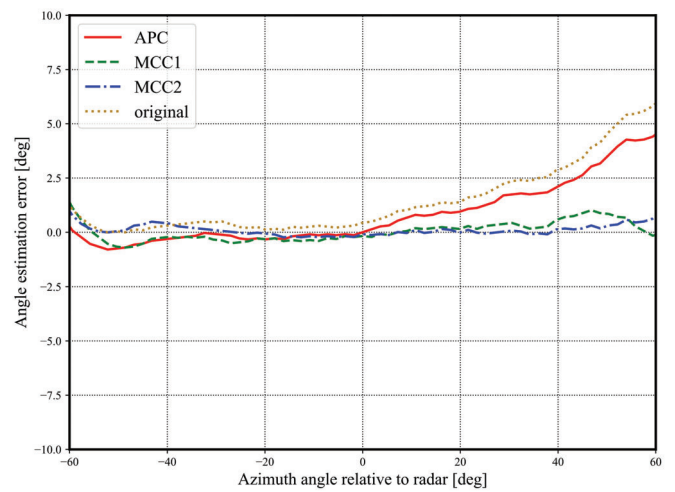


Fig. 7. Angle estimation error before calibration and for different methods.

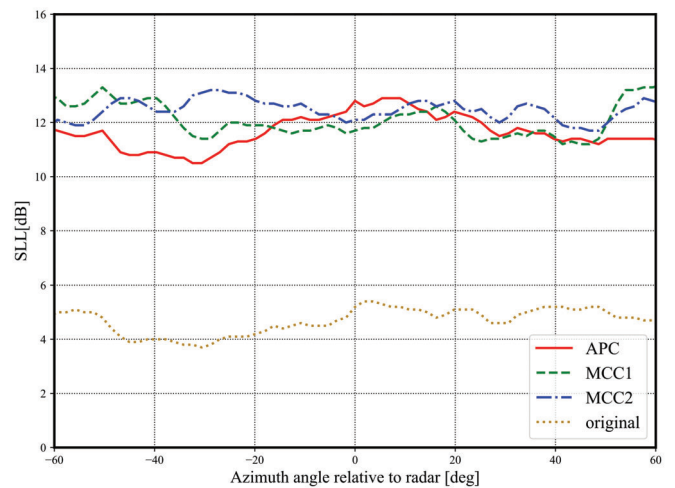


Fig. 8. SLL before calibration and for different methods.

TABLE II
ANGLE ESTIMATION RMSE AND SLL MEAN

	APC	MCC1	MCC2
RMSE _{AOA} [deg]	1.71	0.49	0.31
SLL _{mean} [dB]	11.71	12.15	12.48

B. Different distances

Single target experiments and MCM estimations were done for different distances. In this way it can be examined if MCC is of practical use for estimating AOA of targets at various ranges in the Field Of View (FOV) of the radar. Same radar and same reflector as in section III-A were used, and same sweep of measurements was recorded. Target was placed at distances of 1m and 5m from radar. Calibration matrices estimated in III-A can be applied for calibration. Obtained RMSE_{AOA} and SLL_{mean} for different distances are in Tables III and IV.

TABLE III
ANGLE ESTIMATION RMSE AND SLL MEAN; TARGET AT 1m

	APC	MCC1	MCC2
RMSE _{AOA} [deg]	2.46	0.93	0.97
SLL _{mean} [dB]	11.61	12.16	12.10

TABLE IV
ANGLE ESTIMATION RMSE AND SLL MEAN; TARGET AT 5m

	APC	MCC1	MCC2
RMSE _{AOA} [deg]	2.17	0.69	0.66
SLL _{mean} [dB]	11.67	12.33	12.20

Results show that performing calibration can be done for different distances. Both MCC methods lower RMSE_{AOA} which is only slightly increased for other distances.

C. Different Boards

Estimating MCM is a demanding process, that involves specific equipment and environment. In case calibration has to be done for a large number of devices, it would be impractical to perform the process for each one individually. Measurements of a single target were recorded in the same setup with two different BGT60ATR24C boards. A sweep of measurements in $[-40^\circ, 40^\circ]$ range with 5° step was recorded with both devices. Calibration matrices were calculated in advance. Same matrices were used for calibration of both boards and resulting pseudospectrums are presented in Fig. 9, showing all methods. Pseudospectrums are calibrated and are similar for different boards. This means that MCM estimation for radar devices, can be performed only once. This matrix can then be further used for calibrating other MIMO radar devices in the same production series. When considering the estimation of AOA, MCC for different boards shows almost identical performance. Angle estimation error for two different boards at different angles is given in Fig. 10.

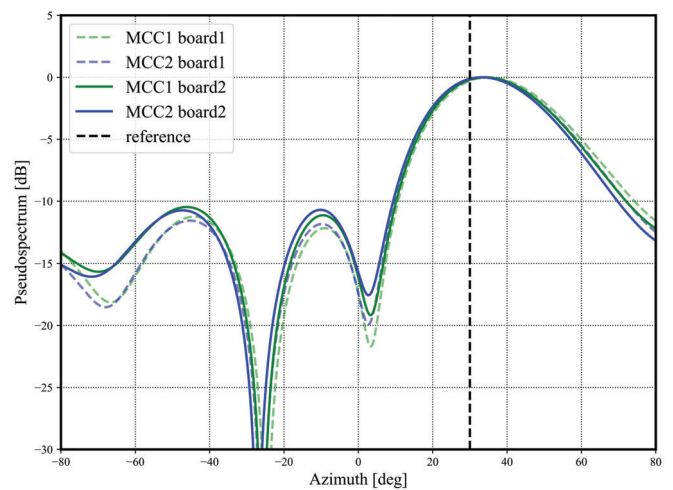


Fig. 9. Angular pseudospectrums for different boards.

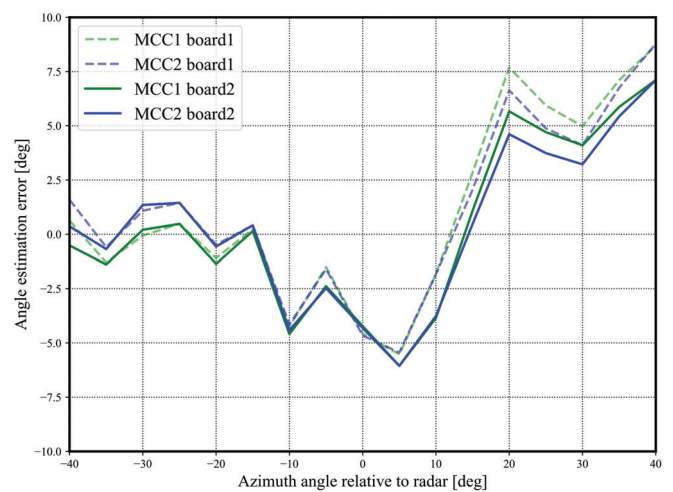


Fig. 10. Angle estimation error for different boards.

D. Experiments with two targets

For better comparison of different calibration methods, it is useful to have a more realistic setup with multiple targets. Two sets of measurements were recorded using both IWR6843 and BGT60ATR24C radars. Two corner reflectors having RCS of 0.26, were placed at various AOAs. Even when multiple targets are present, APC, MCC1 and MCC2 are all successful in calibrating the radar. As demonstrated in Fig. 11 all methods show presence of two targets with great precision for IWR6843 radar. In Table V are RMSE_{AOA} for both targets. These results show that all methods are applicable for scenarios with multiple targets. Using MCC does not significantly improve AOA estimation in this scenario. Same results are considered in Fig. 12 and Table VI for BGT60ATR24C. Larger angle estimation error is present for the case of BGT60ATR24C radar. This is true for all

methods, however error of MCC varies less for different targets. Improvements over APC can be seen as targets in pseudospectrum can be equal in power, as illustrated in Fig. 12.

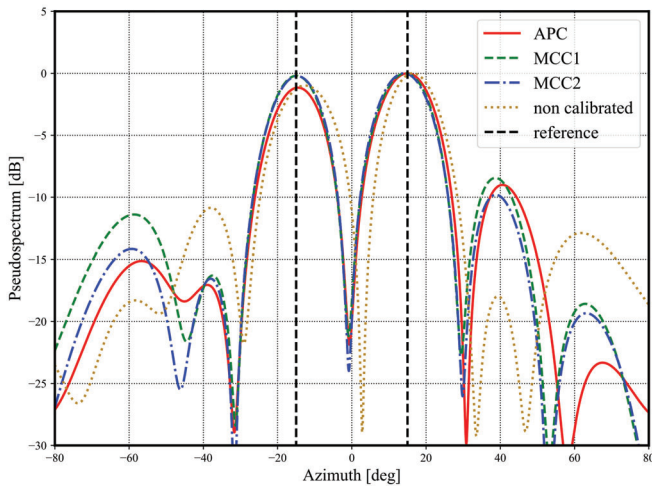


Fig. 11. Angular pseudospectrum with two targets; IWR6843 radar.

TABLE V
ANGLE ESTIMATION RMSE FOR IWR6843 RADAR; TWO TARGETS

		APC	MCC1	MCC2
RMSE _{AOA} left target	[deg]	1.85	2.02	2.03
RMSE _{AOA} right target	[deg]	2.22	2.14	2.18

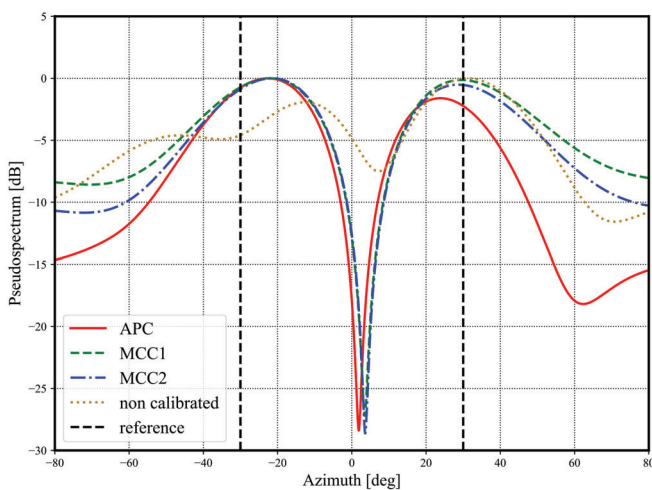


Fig. 12. Angular pseudospectrum with two targets; BGT60ATR24C radar.

TABLE VI
ANGLE ESTIMATION RMSE FOR BGT60ATR24C RADAR; TWO TARGETS

		APC	MCC1	MCC2
RMSE _{AOA} left target	[deg]	4.80	5.03	4.81
RMSE _{AOA} right target	[deg]	11.14	8.49	7.38

IV. CONCLUSION

A comparison of standard APC and MCC is presented. Process of calibration performed by APC and MCC is demonstrated. Procedures for estimating APC coefficients and MCC are described. MCC is generally a more complex operation, requiring more measurements and more sophisticated equipment. The more complex procedure using rotating platform is explained and illustrated. Various datasets were acquired in order to see the performance and benefits of calibration. It is shown that methods can be performed only once, acquiring calibration coefficients and MCCs that can be used for calibration of other radar devices. Experiments at different distances show that calibration performance is reduced, however MCC gives much better angle estimation, especially at angles beyond zero angle. In case of multiple targets, improvements of MCC are not that significant, however MCC can show better performance than APC.

REFERENCES

- [1] M. S. Bartlett, "Smoothing periodograms from time-series with continuous spectra," vol. 161, pp. 686–687, 5 1948.
- [2] J. Capon, "High-resolution frequency-wavenumber spectrum analysis," *Proceedings of the IEEE*, vol. 57, no. 8, pp. 1408–1418, 1969.
- [3] S. Guaning and M. Morf, "The signal subspace approach for multiple wide-band emitter location," *IEEE Transactions on Acoustics, Speech, and Signal Processing*, vol. 31, no. 6, pp. 1502–1522, 1983.
- [4] A. Stove, "Linear FMCW radar techniques," *IEE Proceedings-F*, vol. 139, no. 5, pp. 343–350, 1992.
- [5] H. Krim and M. Viberg, "Two decades of array signal processing research: the parametric approach," *IEEE Signal Processing Magazine*, vol. 13, no. 4, pp. 67–94, 1996.
- [6] H. Steyskal and J. Herd, "Mutual coupling compensation in small array antennas," *IEEE Transactions on Antennas and Propagation*, vol. 38, no. 12, pp. 1971–1975, 1990.
- [7] R. B. Ertel, Z. Hu, and J. H. Reed, "Antenna array hardware amplitude and phase compensation using baseband antenna array outputs," *1999 IEEE 49th Vehicular Technology Conference (Cat. No.99CH36363)*, vol. 3, pp. 1759–1763 vol.3, 1999.
- [8] J. Pierre and M. Kaveh, "Experimental performance of calibration and direction-finding algorithms," in *[Proceedings] ICASSP 91: 1991 International Conference on Acoustics, Speech, and Signal Processing*, pp. 1365–1368 vol.2, 1991.
- [9] C. M. Schmid, R. Feger, C. Wagner, and A. Stelzer, "Mutual Coupling and Compensation in FMCW MIMO Radar Systems," *Frequenz*, vol. 65, no. 9-10, pp. 297–302, 2011.
- [10] M. Mowlér, B. Lindmark, L. Erik, and O. Björn, "Joint estimation of mutual coupling, element factor, and phase center in antenna arrays," *EURASIP Journal on Wireless Communications and Networking*, vol. 2007, 10 2007.
- [11] C. Vasanelli, F. Roos, A. Durr, J. Schlichenmaier, P. Hugler, B. Meinelcke, M. Steiner, and C. Waldschmidt, "Calibration and Direction-of-Arrival Estimation of Millimeter-Wave Radars: A Practical Introduction," *IEEE Antennas and Propagation Magazine*, vol. 62, no. 6, pp. 34–45, 2020.